# MODELING OF STEAM CONDENSATION TRANSIENTS IN THE PITEAS CONTAINMENT TEST FACILITY

Patrick B. **SPITZ**
Institut de Protection et de Sûreté Nucléaire
DRS/SEMAR, Centre d'Etudes de Cadarache
13 115 Saint-Paul lez Durance, FRANCE
&
Sandro **TIRINI**
ENEA, Innovative Reactor Department
via Martiri di Monte Sole, 40100, Bologna, ITALIA

## ABSTRACT

*This paper deals with the assessment of the condensation models (Collier & Chilton-Colburn) and condensation correlations (Uchida & Tagami) implemented in the Jericho code (Escadre System) against three steam condensation transients performed in the Piteas Test Facility, namely SUMPIP A1, A2 & A3. The main purpose is to check the validity of these correlations and models in a condensation transient situation. We analyse the main characteristics of the scenarios of the condensation transients tests SUMPIP A1, A2 & A3 and the experimental results obtained. In order to enhance the predictive capability of the Jericho code, an assessment of condensation models is presented and discussed based on comparisons between Jericho numerical simulations and experimental results. Simply based on the containment mass conservation equation, an analytic modeling is introduced which leads to the calibration of a correlation of the Tagami-Uchida type valid for condensation transient situations.*

## I INTRODUCTION

From the beginning of power plant developments, it has been conceived that a severe accident in which the normal core cooling is lost could lead to fuel element melting with a risk of fission product release beyond the plant limits. In order to contribute to this risk analysis, an in-pile safety research program, namely Phebus Fission Product, is performed by the Institut de Protection et de Sûreté Nucléaire with contributions from the European Community Commission, Japan, Korea, Canada and the United States, at the Research Center of Cadarache (France). The Phebus FP program /1/ offers, as far as possible, a full integration of the phenomena which take place in the core region, the primary system components and the containment building as a result of competing mechanisms in which thermal hydraulic, physical chemical, and radioactive processes are intimately coupled. This program has been mainly designed to obtain experimental reference data to check and qualify the code systems used in the safety analysis for source term evaluation. The Institut de Protection et de Sureté Nucléaire uses the Phebus FP data to assess the Escadre code system.

To analyse the behavior of fission products inside the containment it is necessary to investigate the containment thermal-hydraulics behavior under the experimental conditions. However note that as far as the containment is concerned, the Phebus FP tests are not thermal-hydraulics tests. The aim is to produce particular atmosphere conditions and observe their effects on aerosol behavior and chemistry. Clearly a good code prediction of the humidity ratio is of crucial importance because the deposition rate of aerosols is expected to depend on the relative humidity ratio of atmosphere. Therefore, in the framework of the Phebus FP Program, a Piteas Containment Thermal-Hydraulics Program is run in support to the Phebus FP test preparations. It offers an experimental study of condensation onto simulated reactor containment walls and sump surface in a small scare containment vessel. Both thermal-hydraulic steady state tests and transient tests have been carried out as well as aerosol physics tests /2/.

This paper deals with the assessment of the condensation models (Collier & Chilton-Colburn) and condensation correlations (Uchida & Tagami) implemented in the Jericho code against the three steam condensation transients performed in the Piteas Test Facility, namely SUMPIP A1, A2 & A3. The main purpose is to check the validity of these correlations and models in a condensation transient situation. In a previous paper, a

study was presented on their assessment against thermal-hydraulic steady state test program performed in the Phebus vessel /3/. The Chilton-Colburn model emerged as the best one for predicting experimental data such as total pressure and mass condensation flowrates. A recent paper /4/ analyzing the Phebus FPT0 thermal-hydraulic transient showed weaknesses in the Uchida correlation predictions and an overall best agreement yielded by the Chilton-Colburn model.

In Section II, we briefly present the main characteristics of the Piteas Test Facility together with the scenarios of the condensation transients tests SUMPIP A1, A2 & A3 and the experimental results obtained. In Section III, we outline the Jericho code by describing its general capabilities and the implemented modeling of condensation. In order to enhance the predictive capability of the Jericho code, an assessment of condensation models is presented and discussed, in Section IV, based on comparisons between Jericho numerical simulations and experimental results. Simply based on the containment mass conservation equation, an analytic modeling is introduced in Section V which leads to the calibration of a correlation of the Tagami-Uchida type valid for condensation transients situations. Note that the Tagami-Uchida correlations were obtained for steady state experiments.

## II PITEAS CONDENSATION TRANSIENTS EXPERIMENTS

### II.1 Piteas Test Facility Description

On Figure 1, we present a schematic view of the Piteas containment vessel. It has the following dimensions : overall height = 3.0 m, internal diameter = 1.2 m and a cross section area of 1.1 $m^2$. Its double-skinned structure or double wall cylindrical shell allows the circulation of an organic coolant liquid which is in charge of maintaining an homogeneous gas temperature distribution in its 2.88 $m^3$ . The vessel can be heated up to 160 °C by circulating this organic thermofluid in the 3 sections (top and bottom vaults, cylinder part) which ensure uniform temperatures in the vessel (a typical gas temperature inhomogenety is 0.5 °C). The usual operating pressures range from 3.3 to 5 bar.

A condenser of the Phebus type is attached to the top vault of the Piteas containment vessel. This condenser is in charge of condensing the injected steam and controlling the thermal hydraulic conditions in the vessel. The condensing area is a cylinder of 1.5 m length and 0.15 m diameter. On the condensing surface, the temperature can be controlled by the use of an organic liquid coolant system located inside the cylinder. This system regulates the condenser surface temperature and maintains it to an almost uniform temperature for all the condensing surface. Note that condensed steam is collected in a bottle located in the lower part of the condenser. Located in the lower part of the containment vessel, an injection pipe penetrates the vessel wall in order to introduce steam. A sump that may contain water with a 0.087 $m^2$ surface is located at the bottom vault.

The containment conventional instrumentation is made up atmosphere T-type thermocouples for gas measurements, sump water thermocouples, condenser surface thermocouples for wall measurements, organic coolant thermocouples for temperature control, and a pressure transducer for total pressure measurement. The condensation flow rate is deduced from the information given by the level sensor located inside the water collection bottle which are periodically emptied.

### II.2 Condensation Transient Tests

In this paragraph, we give a short presentation of the condensation transients tests named SUMPIP A1, A2 & A3 performed at the Cadarache Research Center by the IPSN/SREAS/LEA Laboratory. The complete test descriptions are to be found in Sabathier et al. (see references /5, 6 & 7/, available for the Phebus PF Program participants). The initial conditions for each test are summarized in Table I. The test scenario is divided into 3 phases : a preparatory phase during which isothermal tests are performed at about 80 °C and later on at 110 °C (with Twall = Tgas = Tsump) for thermocouple calibration purposes.

| Test SUMPIP | Water Mass (l) | Ptot (bar) | Tgas (°C) | Tsump (°C) |
|---|---|---|---|---|
| A1 | 20 | 0.962 | 22.0 | 22.0 |
| A2 | 20 | 0.958 | 23.4 | 23.4 |
| A3 | 19.8 | 0.972 | 22.9 | 22.9 |

Table I : Initial Test Conditions

A second phase of steam injection of approximately 840 s follows the long preparatory phase in order to reach the targeted thermal-hydraulic conditions. Note that for the SUMPIP A2 test no steam injection was necessary to obtain the pre-defined conditions. The main characteristics of the steam injection phase as well as the final conditions obtained are summarized in Table II.

| SUMPIP Test | A1 | A3 |
|---|---|---|
| Injection Time (s) | 840 | 840 |
| Average Flowrate (g/s) | 1.26 | 1.30 |
| Average Steam Temperature (°C) | 145 | 145 |
| Tgas (°C) - Beginning | 110.4 | 110.0 |
| Tgas (°C) - End | 111.9 | 111.0 |
| Ptot (bar) - Beginning | 2.145 | 2.163 |
| Ptot (bar) - End | 2.703 | 2.742 |
| Pvap (bar) - Beginning | 0.895 | 0.893 |
| Pvap (bar) - End | 1.447 | 1.468 |
| Tsump (°C) - Beginning | 92.0 | 90.0 |
| Tsump (°C) - End | 92.4 | 90.0 |

**Tableau II : Characteristics of Steam Injection Phase**

After a stabilization period of about 600 s, the steam condensation transient proper begins. It is divided into 2 sequences. The first one comprises the period during which the condenser surface temperature is decreased as quickly as possible to a prescribed value. The condensation flowrate will continuously increase during this phase and will be maximum at the end of this first period. The second period lasts until the end of the test. In this situation, we observe the condensation of an initially fixed quantity of steam, so the condensation flowrate will decrease toward zero until the equilibrium partial steam pressure is reached. The latter happens to be the saturation pressure corresponding to the sump free surface temperature. The gas temperature being monitored to an almost constant value, the noncondensable partial pressure is constant so the variation of the total pressure is proportional to the condensation flowrates on condenser and sump. As we will seen later on, the three experiments show that condensation on the sump surface is negligible although the Jericho calculations predict an opposite tendency. The initial conditions of the different condensation phases are :

| SUMPIP Test | A1 | A2 | A3 |
|---|---|---|---|
| Ptot (bar) | 2.671 | 2.178 | 2.710 |
| Pvap (bar) | 1.422 | 0.941 | 1.460 |
| Humidity Rate | 0.98 | 0.66 | * |
| Tgas (°C) | 110.5 | 109.8 | 111.0 |
| Tcond (°C) | 109.8 | 105.3 | 110.0 |
| Tsump (°C) | 92.8 | 89.9 | 90.0 |

**Table III : Initial Conditions of Condensation Phases**

The kinetics of the condenser surface temperature decrease can be considered as linearly depending on time. Their characteristics are listed in Table IV.

| SUMPIP Test | A1 | A2 | A3 |
|---|---|---|---|
| Tcond (°C) - Beginning | 109.8 | 105.3 | 110.0 |
| Tcond (°C) - End | 78.0 | 76.0 | 100.0 |
| Duration (s) | 1 560 | 1 440 | 1 200 |
| Cooling Rate (°C/s) | 0.0204 | 0.0235 | 0.0083 |

**Table IV : Condenser Cooling Characteristics**

The main experimental data recorded during the condensation phases are made up of : the condenser surface temperature versus time, the gas temperature versus time, the sump water temperature, and the total pressure. In the next section, we will describe the way to predict these data using the 0-D Thermal-hydraulics Jericho code.

## III JERICHO CODE SIMULATION OF EXPERIMENTS

### III.1 Outline of the Jericho Code

In the general context of safety analysis, the Institut de Protection et de Sûreté Nucléaire is entrusted with studies related to severe accidents as well as beyond design basis accidents. This assignment has required the development and assessment of a set of codes devoted to studying severe accidents. This system of codes, named Escadre /8/, is in charge of predicting the behavior of a nuclear power plant with water-cooled reactor from the very beginning of core degradation up to fission product release out of containment into the environment. The users are allowed to run codes in a stand-alone or a coupled mode. The Escadre system is mainly divided into two parts : primary circuit codes such as Vulcain, Ecroul, Sophaeros and containment codes such as Jericho, Wechsl, Aerosols-B2 and Iode.

The zero-dimensional Jericho /9/ code enables calculations of containment thermal hydraulics during a severe accident by solving mass and energy balance equations in a pre-defined compartment. The input data consist in the thermal description of containment together with the flow rates of steam and hydrogen. The code calculates pressure and temperature variations in containment as well as the consequence of hydrogen combustion. It is designed for analysis of the thermodynamic evolution of a mixture of non condensable gases and steam in a fixed volume or possibly a multi-compartment one. Pressure and temperature changes in the mixture depend on sources and heat and mass transfers between the confined atmosphere and walls, possibly sump free surface or condensing surfaces as well as other compartments if there are any. The liquid water produced by condensation on walls or by nucleation is instantaneously transferred to the sump. The nucleation is also considered instantaneous, therefore no over saturation is allowed.

### III.2 Modeling of Condensation

The heat and mass transfers during condensation can be optionally chosen by Jericho's users. The following options are available : constant heat transfer coefficient as input parameter, Collier or Chilton-Colburn models and the Uchida correlation. The condensation models of Collier /10/ and Chilton-Colburn, implemented in the Jericho code, write respectively :

$$\dot{m}_c(t) = Kc\ C\ Ms\ Log\left[\frac{Paw}{Pab}\right], \qquad (1)$$

$$\dot{m}_c(t) = Kc\ \left[\frac{\rho_{sw} - \rho_{sat}}{1 - \chi_{sw}}\right], \qquad (2)$$

where the following definitions apply : $\dot{m}_c(t)$ = mass condensation flowrate, $\rho_{sw}$ = steam density near condensing wall, $\rho_{sat}$ = density of saturated steam at condensing surface temperature, Paw = air pressure near condensing wall, Pab = air pressure in bulk, Kc = mass transfer coefficient, C = total molar concentration, $M_s$ = steam molar mass and $\chi_{sw}$ = molar fraction of steam near condensing wall. The main ingredient necessary for both models is an estimate of the mass transfer coefficient Kc (m/s). Actually, it is a key point to a practical use of these models. This coefficient usually writes : $Kc = D/\delta$ where D is the mass diffusivity of steam in air and $\delta$ is a typical length representing for instance a concentration boundary layer. The usual approximation is to obtain the mass transfer coefficient from the classic Chilton-Colburn analogy which relates Kc to the natural convection heat transfer coefficient Hconv in the following way :

$$Kc = Hconv\ Pr^{2/3} / \rho_{bulk}\ Cp\ Sc^{2/3} \qquad (3)$$

with : $P_r$ = Prandtl number of bulk gas, $S_c$ = Schmidt number of bulk gas and Cp = constant pressure specific heat capacity. The values of the total heat transfer coefficient Htot are then computed from the following expressions :

$$Htot = Hconv + Hcond \qquad (4) \qquad Hcond = L\ \frac{1}{(Tgas - Tcond)}\ \dot{m}_c \qquad (5)$$

where L (J/kg) stands for the latent heat of condensation and Tgas and Tcond are respectively the gas and condensing surface temperatures. The convective or sensible heat transfer coefficient Hconv is based on the usual Nusselt expression valid for a turbulent convection regime :

$$Hconv = 0.13\ \lambda\ (Grm\ Pr)^{1/3} \qquad (6)$$

where Grm is related to the Grashof number and writes :

$$Grm = g / v^2\ (1 + (\rho_{sw} + \rho_{aw}) / \rho_{bulk}) \qquad (7)$$

where $\rho_{aw}$ and $\rho_{bulk}$ are respectively the noncondensable density close to the condenser surface and the bulk density. In addition, g is the gravity acceleration, v the bulk kinematics viscosity and $\lambda$ the thermal conductivity. The Uchida and Tagami formulations /11/ adopted in the Jericho code give directly an expression for Htot including convection and condensation contributions, where $\chi$ (dimensionless) stands for the mass ratio of steam to air. They respectively write :

$$Htot\ (W/m^2/K) = 379\ \chi^{0.707} \qquad (8) \qquad Htot\ (W/m^2/K) = 11.3 + 283.8\ \chi \qquad (9)$$

Both correlations allow condensation even if the steam density is lower than the saturation density at the condensing wall temperature. In order to avoid this non-physical behavior, the condensation flow rate is set to zero in the Jericho code when steam density is lower or equal to the saturation value. This procedure may induce abrupt jumps of the heat and mass transfers during the calculation of a transient. We wil suggest in Section V a new formulation avoiding such a drawback.

### III.3 Jericho Simulation of Piteas Containment

The Piteas vessel is modeled with 1 compartment which connects 5 walls : vessel wall, condensing and non condensing parts of the condenser, internal sump wall. In addition, a free sump surface is modeled. The initial conditions are the experimental ones mentioned in Table I. The experimental transient boundary conditions, to be provided as input to the Jericho code, are organic coolant temperature laws. The code linearly interpolates between two organic coolant temperatures. The experimental scenarios are reproduced through the boundary and initial conditions. The values of the steam injection rate and its duration are the experimental ones. The main geometric characteristics and heat transfer coefficients (HTC) between walls and organic liquid coolant are reported in Table V :

| Component | Area ($m^2$) | Wall Thickness (mm) | HTC ($W/m^2/K$) |
|---|---|---|---|
| Vessel Wall | 11.46 | 5.0 | 300 |
| Wet Condenser | 0.775 | 3.5 | 450 |
| Dry Condenser | 0.336 | 3.5 | 450 |
| Wet Sump | 0.254 | 8.0 | 600 |

**Table V : HTC's & Geometric Characteristics**

From previous experiments both carried out in the Piteas /12/ and Phebus /3 & 4/, it was possible to determine from an energy balance during the constant steam injection plateaus the coolant/inner condenser wall HTC's. We came up with the following average value : 450 $W/m^2/K$. The value 300 $W/m^2/K$ has also been estimated against these previous tests. The simulated scenarios have the following characteristics (see Table VI) reproducing the actual experimental sequences.

| PERIOD (s) | SUMPIP A1 | SUMPIP A2 | SUMPIP A3 |
|---|---|---|---|
| Heating 1 | 68 100 | 75 100 | 25 900 |
| Isothermal Test : 80 °C | 1 200 | 1 200 | 50 700 |
| Heating II | 8 700 | 9 600 | 35 700 |
| Isothermal Test : 110 °C | 9 600 | 8 100 | 11 700 |
| Steam Injection | 840 | * | 840 |

| | | | |
|---|---|---|---|
| **Stabilisation** | 560 | * | 660 |
| **Condenser Temperature Decrease** | 1 260 | 1 440 | 500 |
| **Condenser Temperature Stabilized** | 2 300 | 7 560 | 4 000 |

**Table VI : SUMPIP Test Scenarios**

## IV JERICHO/EXPERIMENT COMPARISONS

### IV.1 SUMPIP A1 Test

The objective of a Jericho numerical simulation is to test its predictive capability. In order to do so, we have introduced the known experimental boundary conditions (organic liquid temperature laws) and initial conditions together with the values of the heat exchange coefficients (see Table V). These latter have not been measured but only estimated on previous (unpublished) tests performed in the Piteas containment. The first step for a Jericho/experiment comparison is to check out the consequences of such estimates. In addition, note that boundary temperatures are given with a roughly ± 1.5 °C accuracy.

The condenser surface temperature directly governs the condensation phenomenon we study. On Figure 2, we present a comparison between the experimental and calculated values of the condenser surface temperatures versus time. We focus on the most interesting part of the whole test which starts at the beginning of the injection phase. The assumption made on the condenser organic liquid (O.L.) exchange coefficient leads to a good agreement between the calculated and experimental values. The same remarks can be made on Figure 3 which present a comparison between the sump water calculated and experimental temperatures versus time. When taking into account the ± 1.5 °C accuracy on temperatures and that the liquid temperature depends also on an exchange coefficient wall/liquid in addition to the O.L./wall exchange coefficient, the comparison is excellent. For the vessel gas temperature, the wall/gas exchange coefficient is modelled by the classic Mac Adam correlation (see eq. 6). The result of the predicted and experimental gas temperatures versus time is displayed on Figure 4. The code predicts the experimental slight decrease during the first part of the condensation phase and its stabilization during the second phase. The overall agreement is again very good. The success obtained in reproducing correctly the gas, condenser surface and liquid temperatures induces more confidence in the total pressure comparison which is the key point to the interpretation of the SUMPIP tests.

The latter were designed as attempts to test condensation transients in the Piteas vessel. The presence of a sump full of water was necessary for evaporation (SUMPIP A2) but was also another condensing surface. Previous tests have demonstrated that condensation on the Piteas sump surface was completely negligible due to probably the presence of a stable layer of air non disturbed by natural convection vessel wall and condenser. On the other hand, the stable air layer is only destabilized in case of evaporation. The prediction of a correct relative humidity rate in the Phebus tests is a crucial point. The humidity rate is essentially governed by the mass condensation rate whose correct prediction becomes in turn very important. In the SUMPIP tests, the total pressure variation is directly proportional to the mass condensation flowrate assuming an ideal gas behavior of the air/steam mixture and the knowledge of the air partial pressure from the initial condition. This rationale reports all the information we are seeking on the time behavior of the total pressure during the experimental transients. That is the reason why in the following we concentrate on the numerical predictions of the total pressure given by the models and correlations implemented in the Jericho code. In addition, the total pressure is generally an easy measurement to perform with a very good accuracy on the results.

On Figure 5, the experimental values of the total pressure is compared to the ones obtained with the Chilton-Colburn and Collier models and the Uchida correlation. Despite the introduction in the simulation of the exact steam injection rate and duration, we do not obtain the same level of total pressure. The reason is because the code condenses water on the sump surface (0-D code simulation) during the steam injection whereas this phenomenon is inhibited in the Piteas vessel. The total pressure decreases slowly during the stabilization phase. Again, the Jericho code reproduces this behavior but for a lower level of pressure. From a simulation point of view the reason is clearly explained by condensation on the sump surface which decreases as time passes by. However, the experimenters suggest that this 0.03 bar decrease of pressure could be attributed mainly to an homogenization of the air/steam mixture coupled to a very negligible amount of condensation on the sump surface. For the condensation phase proper, the best overall agreement is obtained with the Chilton-Colburn model as already noticed and mentioned in /3 & 4/. The Collier model gives also a good prediction of the total pressure values

together with the same physical behavior as the experimental one. The calculated/experimental pressure difference increases for both models and reaches its maximum at the end of the test : we get approximately for the Chilton-Colburn and Collier models 1.5 and 4 % pressure difference underpredictions based on the experimental values. The result given by the Uchida correlation is not satisfactory because it is highly unphysical. At the end of the condenser surface temperature decrease toward its constant value, the predicted pressure has already reached the equilibrium pressure which should be met at the end of the test although the pressure difference is under estimated (10 %). During the second phase of condensation, the total pressure remains almost constant. Again, this unphysical behavior have been noticed in references /3 & 4/.

### IV.2 SUMPIP A2 Test

For this test, no steam injection was necessary to reach the prescribed values for total pressure at the beginning of condensation phase. On Figure 6, we present a comparison between the experimental and calculated values of condenser surface temperatures versus time. As for the SUMPIP A1 test, the assumption made on condenser O.L. exchange coefficients leads to a very good agreement between the calculated and experimental values. Figure 7 presents a comparison between the sump water calculated and experimental temperatures versus time. The agreement turns out to be excellent which is important because in this case the steam production is yielded by sump evaporation. The result of the predicted and experimental gas temperatures versus time is displayed on Figure 8. The overall agreement is excellent when considering the measurement accuracy of atmosphere thermocouples.

On Figure 9, the experimental values of the total pressure is compared to the ones obtained with the Chilton-Colburn and Collier models and the Uchida correlation. The reference time t = 0 was chosen at the end of the preparatory phase which was a sump evaporation. We notice on Figure 9 a strong discrepancy between the calculated and measured values. As remarked by the experimenters /6/, the saturation pressure corresponding to a 90°C sump temperature is 0.7 bar and the noncondensable pressure at 110 °C is about 1.24 bar. Therefore the total pressure should be 1.94 bar (which is the Jericho code result also) whereas the experimental value is 2.10 bar. The experimental data are affected by a calibration error during the first thousand seconds. However, during the second condensation phase (starting at about 1 400 s), the same behaviors as those noticed in the SUMPIP A1 test are observed. Again, the best overall agreement is obtained with the Chilton-Colburn model. The Collier model gives also a good prediction of the total pressure values together with the same physical behavior as the experimental one. The calculated/experimental pressure difference increases for both models and reaches its maximum at the end of the test : we get approximately for the Chilton-Colburn and Collier models - 4 and - 5 % pressure difference underpredictions based on the experimental values. As expected now, the result given by the Uchida correlation is not satisfactory. At the end of the condenser surface temperature decrease toward its constant value, the predicted pressure has already reached the equilibrium pressure which should be met at the end of the test although the pressure difference is roughly -7 %. During the second phase of condensation, the total pressure remains almost constant. This comparison suggests that the experimental data during this condensation phase does not suffer from the same measurement error and then will be able to be integrated in the data fit presented in Section V.

### IV.3 SUMPIP A3 Test

On Figure 10, we present a comparison between the experimental and calculated values of the condenser surface temperatures versus time. As in the SUMPIP A1 test, we concentrate on the most interesting part of the whole test which starts at the beginning of the injection phase. The experimental temperature decrease is very correctly reproduced by the Jericho simulation. The result of the predicted and experimental gas temperatures versus time is displayed on Figure 12. The code predicts the experimental gas temperature variations during the whole transient and when taking into account the experimental error band the overall agreement is excellent.

A difficulty happens when we consider the comparison on sump water temperatures (Figure 11). The experimental behavior shows a slight tendency to a temperature increase (1 °C) during the transient although it is comprised within the sump thermocouple error band. The Jericho simulation behavior is quite different in that the sump temperature increases strongly (up to 3 °C) and then decreases down to 91 °C. The explanation comes from Figure 16 which displays the calculated condensation flowrates on the condenser and sump surfaces. Because the condenser surface is at 100 °C and the sump surface at 90 °C, this latter plays the major role in condensation. The condenser acts during a period of 1 400 s in the simulation then stops acting. In summary, the calculation simulates a scenario where condensation is mainly onto the free sump surface whereas the experimental scenario demonstrates that condensation acts onto the condenser due to an inhibition of condensation over the sump free

surface. As a matter of fact, the impossibility of simulating the SUMPIP A3 test with a sump surface at 90 °C is an extra proof of the passiveness of the sump. The SUMPIP A3 test is a condensation transient test on the condenser surface only. The only way of correctly predicting the experimental data is to suppress the presence of the sump in the Jericho code. The simulation has been done but the results will not be presented here. According to the foregoing explanations, one can understand the frank discrepancy on the total pressure comparison presented on Figure 13. Nevertheless, the conclusion that these data can be used for a correlation fit is easily drawn.

## V THEORETICAL MODELING OF CONDENSATION TRANSIENTS

### V.1 Modeling of Condensation

As previously mentioned, after a stabilization period of about 600 s, the steam condensation transient proper begins at time $t_0$. It is divided into 2 sequences. The first one comprises the period during which the condenser surface temperature is decreased as quickly as possible to a prescribed value, noted $t_1$. The second period lasts until the end of the test. In this situation, we observe the condensation of an initially fixed quantity of steam, so the condensation flowrate will decrease toward zero until the equilibrium partial steam pressure is reached at time $t_2$ which happens to be the saturation pressure corresponding to the sump free surface temperature. The gas temperature being maintained to an almost constant value, the noncondensable partial pressure is almost constant so the variation of the total pressure is proportional to the condensation flowrates on condenser and sump. The observed condensation phenomenon (video filming) shows a droplet formation on the upper part of the condensing surface and a droplet coalescence on the lower part leading merging to yield rivulets without the generation of an observable condensation film. That is why we shall restrict ourselves to an overall correlation approach with no reference to any condensation film properties.

We suggest the following modeling for the steam pressure in the Piteas containment or, in other words, a model for the steam condensation rate. We first model the condensation heat transfer Hcond ($W/m^2/K$) with an Uchida-type correlation of the form :

$$Hcond = a\,[\chi\,(t) - \chi^*\,(t)]^{\,b} \qquad (10)$$

where a ($W/m^2/K$) and b (dimensionless) are 2 unknown model parameters and $\chi$ (t) is the steam (ms) to air (ma) mass ratio in containment versus time such as :

$$\chi = \frac{ms\,(t)}{ma} \qquad \chi^* = \frac{ms^*\,(t)}{ma} \qquad (11)$$

where ms* (t) = steam mass corresponding to a steam partial pressure equal to the steam saturation pressure at Tcond (t). Taking into account eq. (10), the condensation flowrate $\dot{m}c(t)$ (see eq. 5) writes :

$$\dot{m}c\,(t) = \frac{S}{L}\,(Tgas - Tcond\,(t))\,Hcond \qquad (12)$$

where S is the condensing area of condenser. Neglecting condensation on the sump free surface, the mass conservation of steam in containment (noncondensable mass ma is constant) writes :

$$\frac{d}{dt}ms\,(t) = -\,\dot{m}c\,(t) \qquad (13)$$

Inserting eqs. (10) & (12) in eq. (13), one obtains :

$$\frac{d}{dt}\chi(t) + \frac{S\,a}{L\,ma}\,[Tgas - Tcond\,(t)]\,[\chi\,(t) - \chi^*(t)]^b = 0 \qquad (14)$$

The two variables Tcond (t) and $\chi^*(t)$ depend on time during the first part of the condensation transient (from $t_0$ to $t_1$) and are constant during the second part (from $t_1$ to $t_2$) and tend to equilibrium values Tce and $\chi^* e$ (we neglect the time variations of the latent heat condensation). This suggests to make appear these constant values by proceeding to the following substitutions which turn out to be the definition relations for the dimensionless functions $\phi$ (t) and $\psi$ (t) :

$$Tgas - Tcond\,(t) = (Tgas - Tce)\,\phi\,(t) \qquad \text{and} \qquad \chi(t) - \chi^*(t) = (\chi(t) - \chi^* e)\,\varphi(t) \qquad (15)$$

Combining the physical parameters associated with eq. (14), one can obtain the characteristic time $\tau$ associated with the condensation phenomenon at hand. This characteristic time writes :

$$\tau = \frac{L\,ma}{S\,a\,(Tgas - Tce)} \qquad (16)$$

The last step is to insert eqs. (15) & (16) into eq. (14) to obtain the model equation we are looking for which writes :

$$\frac{d}{dt}\chi(t) + \frac{1}{\tau}[\chi(t) - \chi^{*}e]^{b}\,\phi(t)\,\psi^{b}(t) = 0 \qquad (17)$$

**V.2 Variable Condenser Surface Temperature**

First, we look for a solution to eq. (17) when the condenser surface temperature varies in-between $t_0$ and $t_1$ . We define a dimensionless time $\omega$ and mass fraction F such as :

$$\omega = \frac{t - t_0}{t_1 - t_0} \quad \text{and} \quad F = \frac{\chi - \chi_1}{\chi_0 - \chi_1} \qquad (18)$$

where $\chi_0 = \chi(t_0)$ and $\chi_1 = \chi(t_1)$ . Next, we model the dimensionless functions $\phi$ (t) and $\psi$ (t) versus $\omega$ by assuming a linear variation of the condenser surface temperature between its starting and final values and a variation of $\psi$ depending on some power of $\omega$. The foregoing assumptions write :

$$\phi(\omega) = \omega \quad \text{and} \quad \psi(\omega) = \omega^{m} \qquad (19)$$

For instance, an evaluation of m against the SUMPIP A1 test yields m = 0.5 (see Figure 18). Inserting eqs. (18) and (19) into (17), one obtains :

$$\frac{d}{d\omega}F + \frac{\Delta}{\tau}[\chi_0 - \chi_1]^{b-1}[F + \lambda]^{b}\,\omega^{(1+mb)} = 0 \qquad (20)$$

where $\Delta = t_1 - t_0$ and $\lambda = (\chi_1 - \chi^{*}_e) / (\chi_0 - \chi_1)$. Then the solution to eq. (20) writes :

$$\left[\frac{\lambda + F}{\lambda + 1}\right]^{1-b} = 1 + \left[\left(\frac{\lambda}{\lambda + 1}\right)^{1-b} - 1\right]\omega^{2+mb} \qquad (21)$$

The integration constant is evaluated from the condition F (0) = 1. Use is also made of the compatibility condition stemming from F(1) = 0.

**V.3 Constant Condenser Surface Temperature**

In this case, the solution to eq. (17) is much simpler than eq. (21) and more easily tractable for data fitting. For $t_1 < t < t_2$ , eq. (17) reduces to :

$$\frac{d}{dt}\chi(t) + \frac{1}{\tau}[\chi(t) - \chi^{*}e]^{b} = 0 \qquad (22)$$

Assuming again for convenience, the following dimensionless forms for time and mass fraction :

$$\omega = \frac{t - t_1}{t_2 - t_1} \quad \text{and} \quad F = \frac{\chi - \chi^{*}_e}{\chi_1 - \chi^{*}_e} \qquad (23)$$

where we assume $\chi(t_2) = \chi^{*}e$ and inserting this latter into eq. (22), one obtains :

$$F(\omega) = \left[1 - (1 - b)\frac{t_2 - t_1}{\tau}(\chi_1 - \chi_{*e})^{b-1}\omega\right]^{\frac{1}{1-b}} \qquad (24)$$

where the integration constant is evaluated from F (0) = 1. The assumption that a time $t_2$ can be defined such as $\chi(t_2) = \chi^{*}e$ implies F (1) = 0 or from eq. (24) we get the compatibility equation :

$$[\chi_1 - \chi^{*}_e]^{b-1} = \frac{\tau}{(t_2 - t_1)(1 - b)} \qquad (25)$$

When accounting for the latter, eq. (24) writes simply :

$$F(\omega) = [1 - \omega]^{\frac{1}{1-b}} \qquad (26)$$

**V.4 Comparison with Experiments**

A direct comparison with the SUMPIP experiments is then possible using eq. (26). The latter re-writes as following, PT (t) being the total vessel pressure :

$$F(\omega) = \frac{P_T(t) - P_T(t_2)}{P_T(t_1) - P_T(t_2)} = \left[\frac{t_2 - t}{t_2 - t_1}\right]^{\frac{1}{1-b}} \qquad (27)$$

We represent on Figures 17, 19 & 20 the evolutions of eq. (26) based respectively on SUMPIP A1, A2 & A3 total pressure measurements. The main values of parameters are summarized in Table VII :

| SUMPIP Test | A1 | A2 | A3 |
|---|---|---|---|
| $t_1$ (s) | 2 700 | 1 300 | 1 850 |
| $t_2$ (s) | 5 000 | 3 400 | 4 200 |
| PT ($t_1$) (bar) | 2.067 | 1.915 | 2.638 |
| PT ($t_2$) (bar) | 1.732 | 1.721 | 2.422 |
| b | 0.615 | 0.565 | 0.629 |

**Table VII : Data Fit of Correlation Exponent b**

The determination of the corresponding a values is more delicate. From eqs. (16) and (25), the following expression can be derived :

$$a = \frac{m\ a\ L\ (Tce)\ (\chi_1 - \chi^*_e)^{1-b}}{(1 - b)\ S\ (Tgas - Tce)\ (t_2 - t_1)} \qquad (28)$$

Inserting the experimental values in eq. (28), one obtaind the following results summarized in TableVIII :

| SUMPIP Test | a ($W/m^2/K$) |
|---|---|
| A1 | 190 |
| A2 | 160 |

**Table VIII : Determination of Correlation Parameter a**

When taking into account the experimental error which can be estimated as being about 10% at least, the a-values show some natural discrepancy. We have discarded the A3 experiment in the evaluation of the a-value because of a large uncertainty on the air mass in this case value which plays an important role (see eq. (28)). Nevertheless the experiments A1 & A2 allow a reliable determination of the corresponding a-values and we can propose, at the moment, an average value such as : a = (175 ± 20) W/m2/K. The presence of the sump might be disturbing in the assessment of a condensation correlation, so a study is being performed on similar tests run without the sump and will be published later on. Summarizing the correlation data fit on the SUMPIP experiment, we obtain :

$$Hcond = 175\ [\chi(t) - \chi^*(t)]^{0.6}$$

## VI CONCLUDING REMARKS

This paper deals with the assessment of the condensation models implemented in the Jericho code against the steam condensation transients namely SUMPIP A1, A2 & A3 performed in the Piteas Test Facility. The main objective is to check the validity of these models in a condensation transient situation. In order to enhance the predictive capability of the Jericho code, an assessment of condensation models is presented and discussed, based on comparisons between Jericho numerical simulations and experimental results. For the condensation phase proper of the SUMPIP tests, the best overall agreement is obtained with the Chilton-Colburn model as already noticed in previous papers for steady-state situations. The Collier model gives also a good prediction of the total pressure values together with the same physical behavior as the experimental one. The result given by the Uchida correlation is not satisfactory because it is highly unphysical. At the end of the condenser surface temperature decrease toward its constant value, the predicted pressure has already reached the equilibrium pressure which should be met at the end of the test although the pressure difference is under estimated (10 %). Again, this unphysical behavior have been previously reported. Simply based on containment mass conservation equation, an analytic modeling of the condensation flowrate (or the condensation heat transfer) is proposed. This modeling consists of overall correlation approach with no reference to any

condensation film properties. Actually the observed condensation phenomenon shows a droplet formation on the upper part of the condensing surface and a droplet coalescence on the lower part leading merging to yield rivulets without the generation of an observable condensation film. The assessment of the proposed correlation against the SUMPIP tests involves the calibration of two model parameters. The determination of the a-parameter shows some dispersion due to experimental data scattering. We propose the following form to correlate the condensation heat transfer coefficient Hcond (W/m2/K) for a closed vessel in the presence of noncondensable gases :

$$Hcond = 175\ [\chi\ (t) - \chi^{*}\ (t)]^{0.6}$$

The presence of the sump being disturbing in the assessment of a condensation transient correlation, a study is underway, at the present time, on similar tests run without the presence of water in the sump. We intend to assess definitively the a and b parameter values against these tests.

## REFERENCES


/1/ M. SCHWARZ and P. von der HARDT, « The Severe Accident Research Programme Phebus FP : First Results and Future Tests »,23rd Water Reactor Safety Information Meeting, Bethesda, MD, USA, October 23-25, 1995.

/2/ F. SABATHIER, T. ALBIOL & A. ZOULALIAN, « Piteas Experiments : the Growth of Hygroscopic Aerosol in Humid Atmosphere », 3rd International Conference on Containment Design and Operation, Toronto, Canada, October 19-21, 1994.

/3/ P. SPITZ, V.D. LAYLY, S. TIRINI & A. MAILLIAT, « A review of Some Phebus Fission Product Containment Thermal-hydraulic Results and their Applications to Jericho Code Assessment », Int. Conf. on New Trends in Nuclear System Thermohydraulics, Pisa, Italy, May 30th - June 2nd , 1994.

/4/ V. D. LAYLY, P. SPITZ, S. TIRINI & A. MAILLIAT, « Analysis of the Phebus FPT0 Containment Thermal Hydraulics with the Jericho and Trio-VF Code », 3rd International Conference on Containment Design and Operation, Toronto, Canada, October 19-21, 1994.

/5/ M. BLANCHARD, Y. MARTINEZ & F. SABATHIER, « Premier Essai Sumpip dans l'Installation Piteas : SUMPIP A1 », Internal Report IPSN/DRS/SREAS/LEA N° 95/608, June 9, 1995.

/6/ M. BLANCHARD, Y. MARTINEZ & F. SABATHIER, « Deuxième Essai Sumpip dans l'Installation Piteas : SUMPIP A2 », Internal Report IPSN/DRS/SREAS/LEA N° 95/929, August 8, 1995.

/7/ M. BLANCHARD, Y. MARTINEZ & F. SABATHIER, « Troisième Essai Sumpip dans l'Installation Piteas : SUMPIP A3 », Internal Report IPSN/DRS/SREAS/LEA N° 95/999, August 22, 1995.

/8/ A. MAILLIAT, C. RENAULT & B. SCHWINGES « Escadre mod0 and Raloc mod2 Assessment. Major Findings and Relevance to the Safety of LWR's »,International Seminar on Heat and Mass Transfers in Severe Reactor Accidents, May 22-26, 1995. CESME, IZMIR, TURKEY.

/9/ J. GAUVAIN and J. P. L'HERITEAU, « Escadre System : Jericho code release 2.4 - Reference Document », Internal Report, IPSN/DEAC/91-05 - 1991

/10/ J. G. COLLIER, « Convective Boiling and Condensation », Mac Graw Hill Book Company, pp. 311 - 314, 1972

/11/ M. H. KIM and M. L. CORRADINI, « Modeling of condensation heat transfer in a reactor containment », Nuclear Engineering and Design 118, pp. 193 - 212, North-Holland - 1990.

/12/ V-D LAYLY, P. SPITZ & S. TIRINI, « Validation du Code Jericho : Analyse des Essais Thermohydrauliques PITEAS », Internal Report IPSN/DRS/SEMAR/LPA 95/13 - 1995

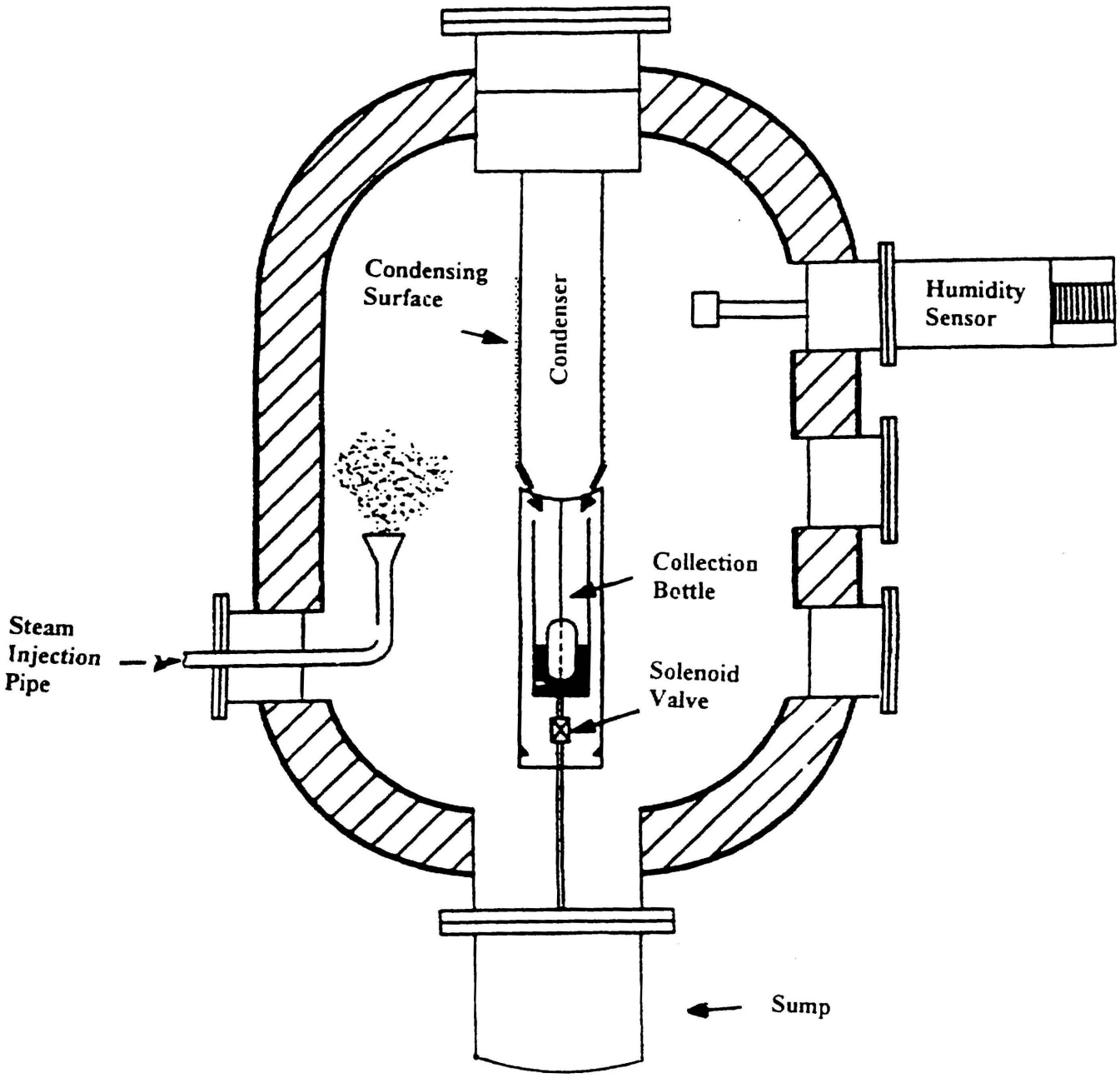


PITEAS FACILITY – SUMPIP TESTS

Fig. 1 – SCHEMATIC VIEW OF THE PITEAS FACILITY

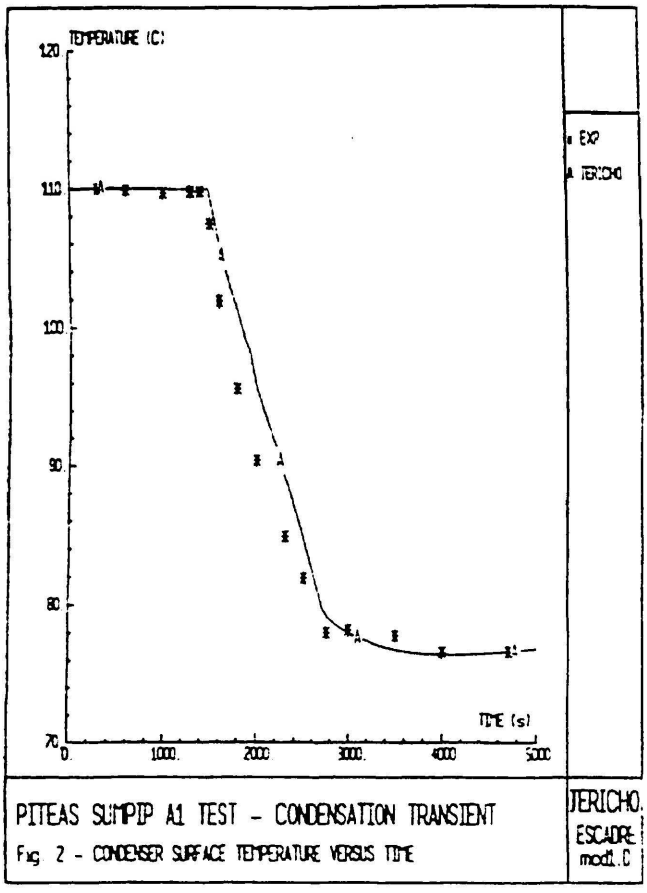


PITEAS SUMPIP A1 TEST - CONDENSATION TRANSIENT

Fig. 2 - CONDENSER SURFACE TEMPERATURE VERSUS TIME

JERICHO
ESCADRE
mod1.0

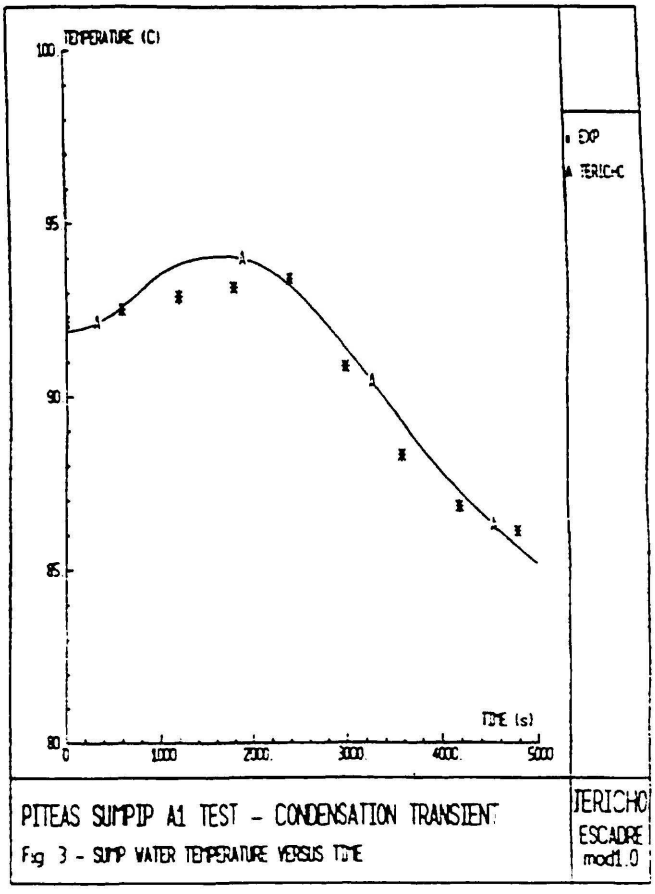


PITEAS SUMPIP A1 TEST - CONDENSATION TRANSIENT

Fig 3 - SUMP WATER TEMPERATURE VERSUS TIME

JERICHO
ESCADRE
mod1.0

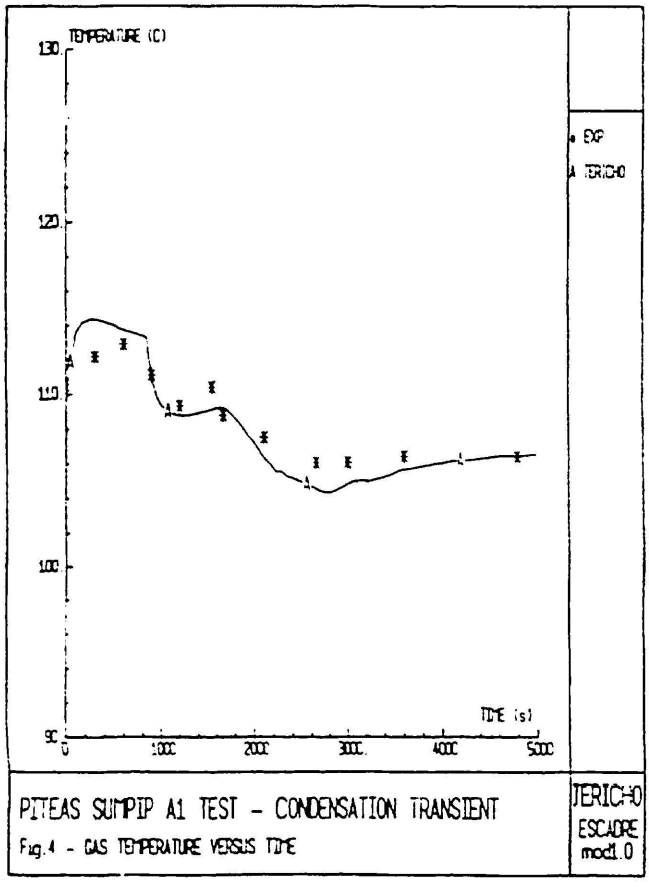


PITEAS SUMPIP A1 TEST - CONDENSATION TRANSIENT

Fig.4 - GAS TEMPERATURE VERSUS TIME

JERICHO
ESCADRE
mod1.0

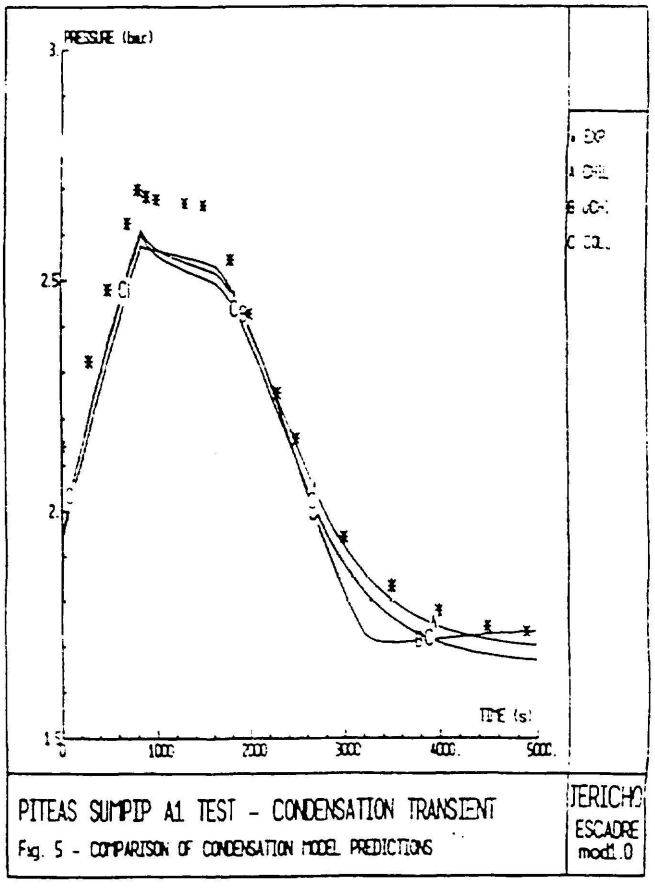


PITEAS SUMPIP A1 TEST - CONDENSATION TRANSIENT

Fig. 5 - COMPARISON OF CONDENSATION MODEL PREDICTIONS

JERICHO
ESCADRE
mod1.0

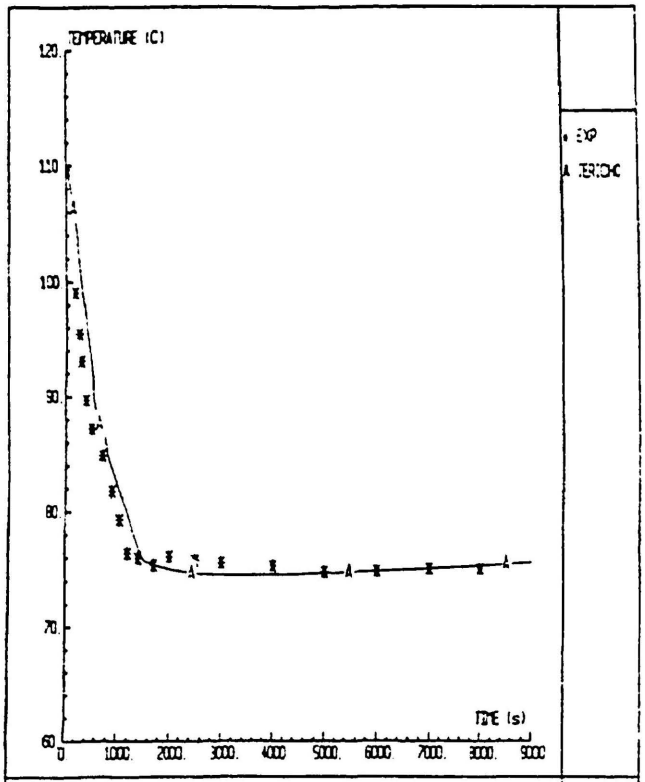


PITEAS - SUMPIP A2 TEST - CONDENSATION TRANSIENT

Fig. 6 - CONDENSER SURFACE TEMPERATURE VERSUS TIME

JERICHO
ESCADRE
modl.0

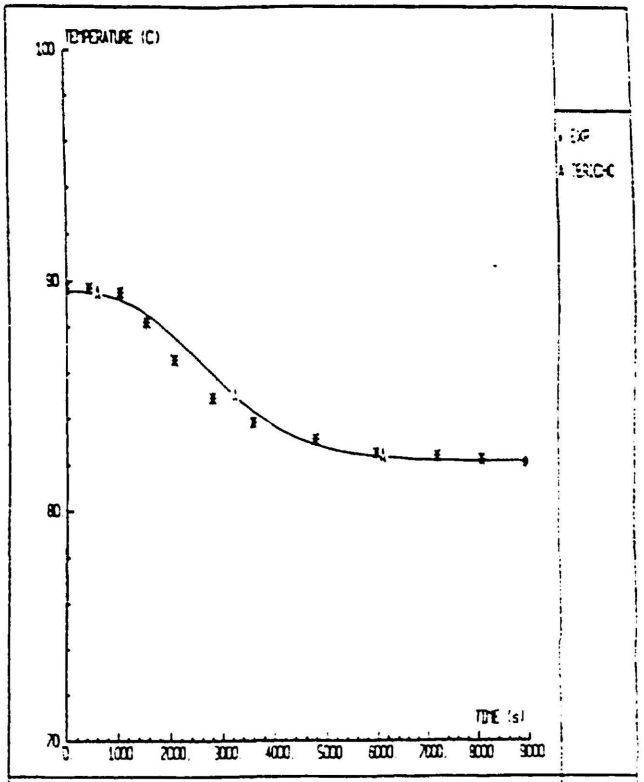


PITEAS - SUMPIP A2 TEST - CONDENSATION TRANSIENT

Fig. 7 - SUMP WATER TEMPERATURE VERSUS TIME

JERICHO
ESCADRE
modl.0

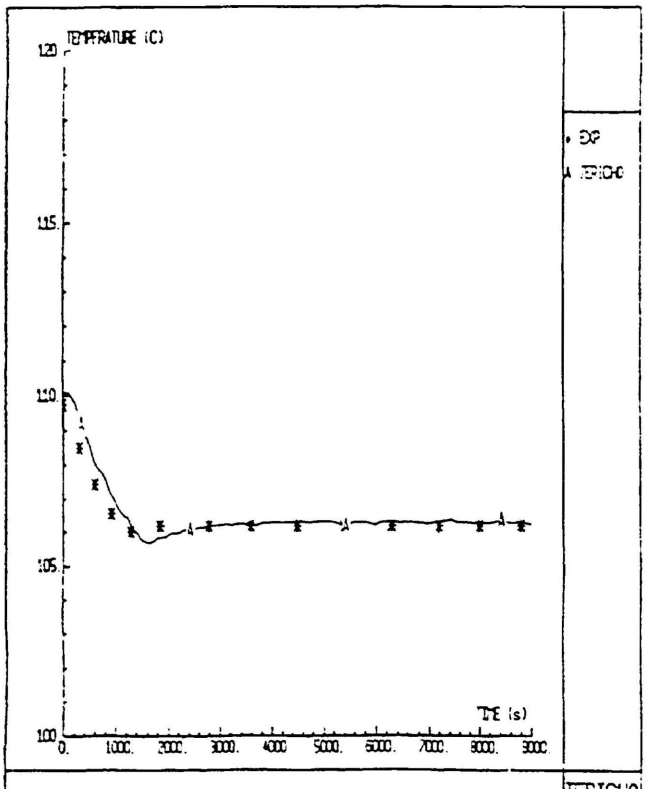


PITEAS - SUMPIP A2 TEST - CONDENSATION TRANSIENT

Fig. 8 - GAS TEMPERATURE VERSUS TIME

JERICHO
ESCADRE
modl.0

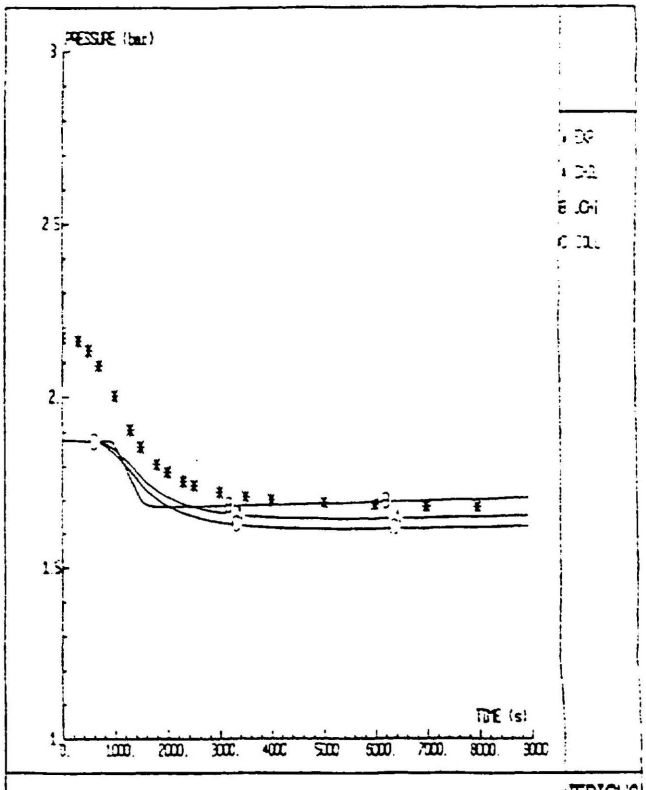


PITEAS - SUMPIP A2 TEST - CONDENSATION TRANSIENT

Fig. 9 - COMPARISON OF CONDENSATION MODEL PREDICTIONS

JERICHO
ESCADRE
modl.0

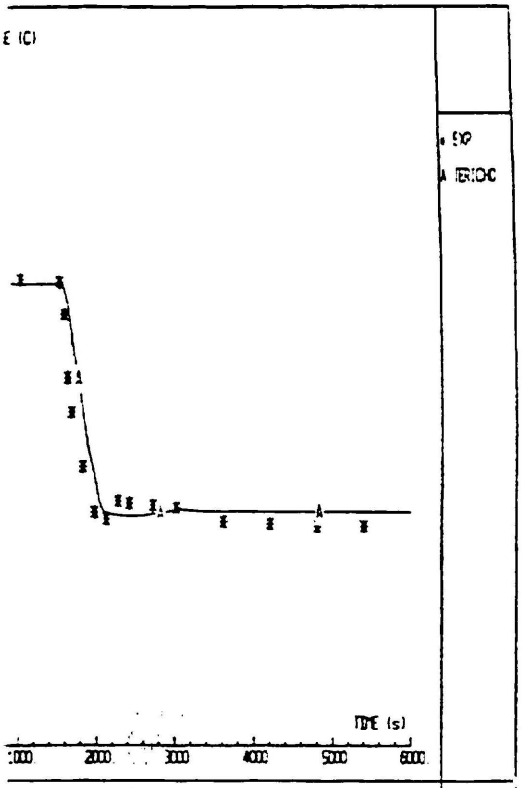


:MPIP A3 TEST - CONDENSATION TRANSIENT
:DSER SURFACE TEMPERATURE VERSUS TIME

JERICHO
ESCADRE
modl.0

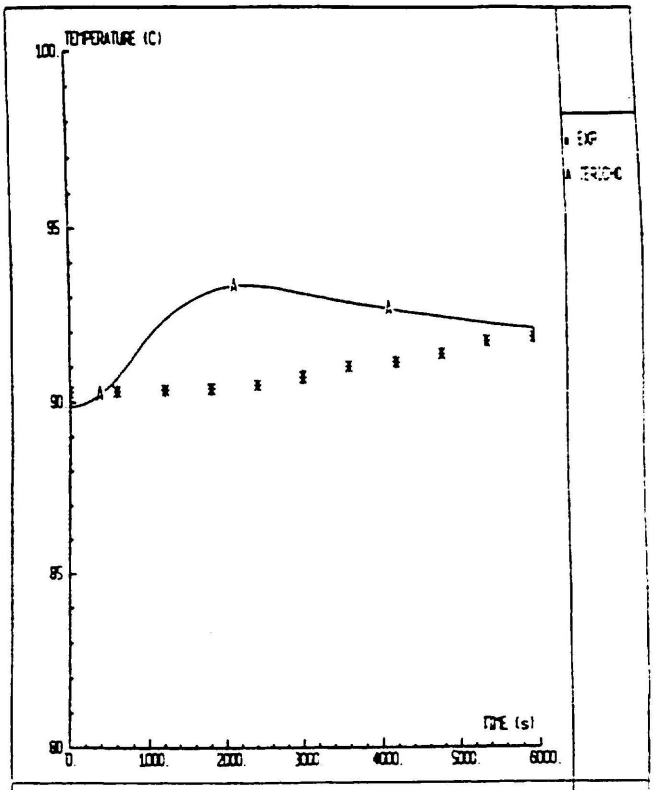


PITEAS - SUMPIP A3 TEST - CONDENSATION TRANSIENT
Fig 11 - SUMP WATER TEMPERATURE VERSUS TIME

JERICHO
ESCADRE
modl.0

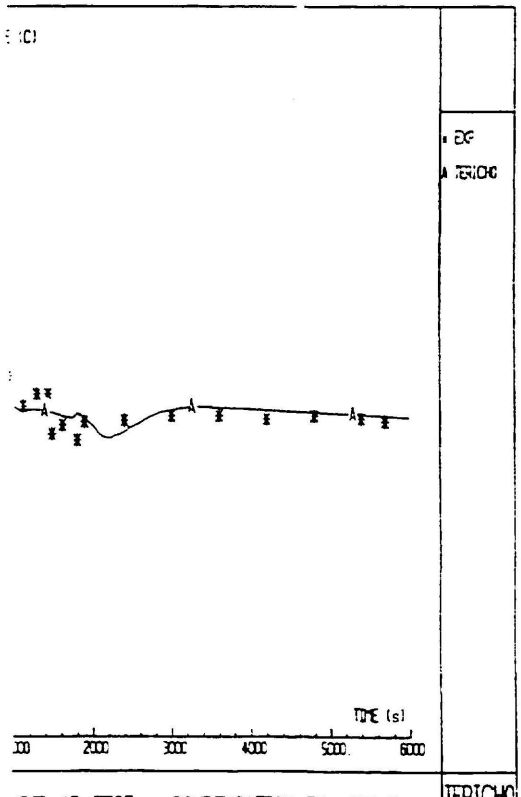


'MPIP A3 TEST - CONDENSATION TRANSIENT
'PERATURE VERSUS TIME

JERICHO
ESCADRE
modl.0

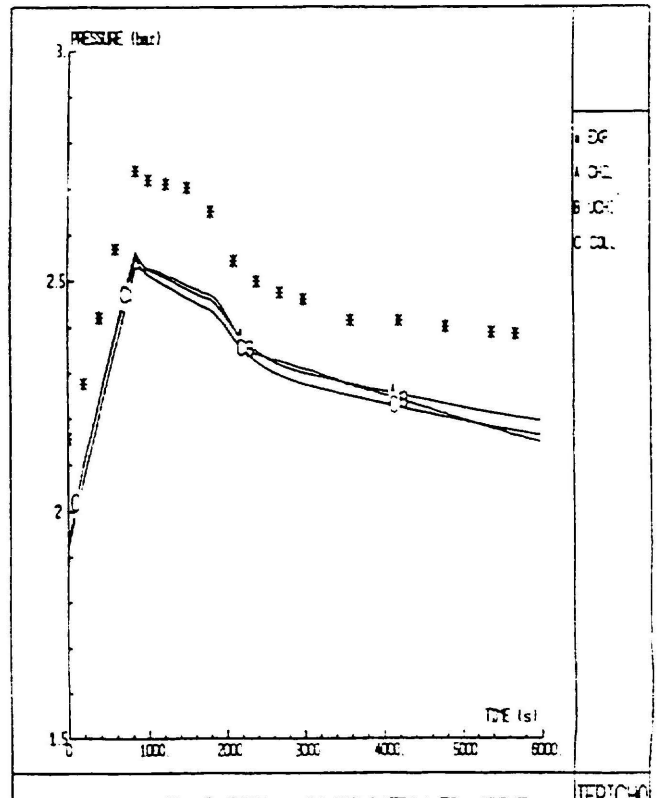


PITEAS - SUMPIP A3 TEST - CONDENSATION TRANSIENT
Fig.13 - COMPARISON OF CONDENSATION MODEL PREDICTIONS

JERICHO
ESCADRE
modl.0

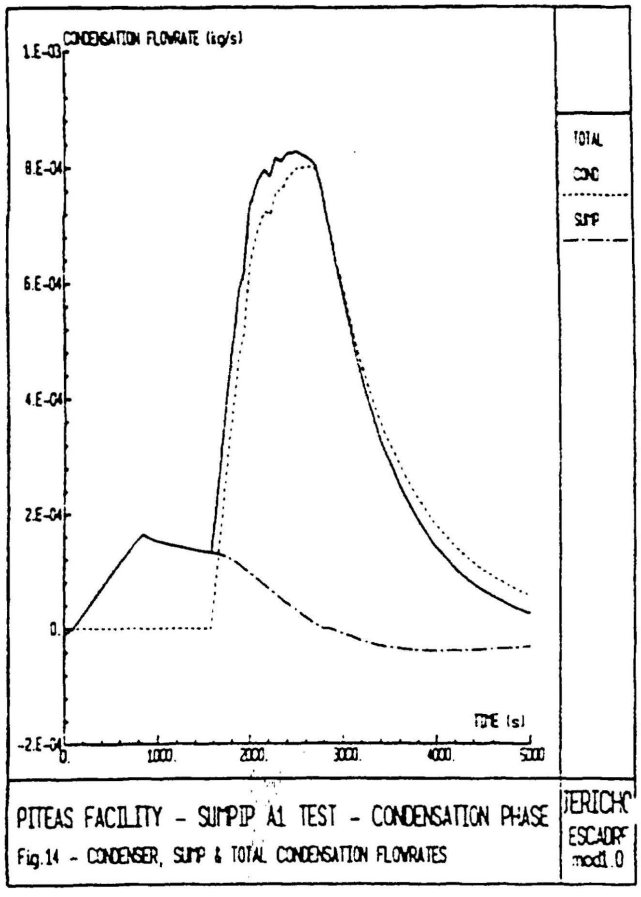


PITEAS FACILITY - SUMPIP A1 TEST - CONDENSATION PHASE

Fig.14 - CONDENSER, SUMP & TOTAL CONDENSATION FLOWRATES

JERICHO
ESCADRE
mod1.0

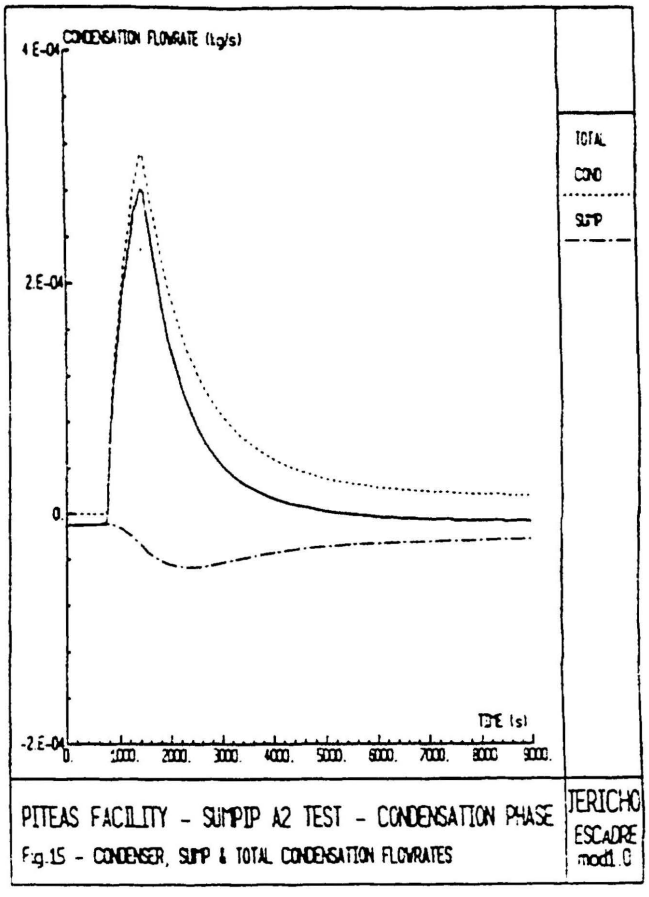


PITEAS FACILITY - SUMPIP A2 TEST - CONDENSATION PHASE

Fig.15 - CONDENSER, SUMP & TOTAL CONDENSATION FLOWRATES

JERICHO
ESCADRE
mod1.0

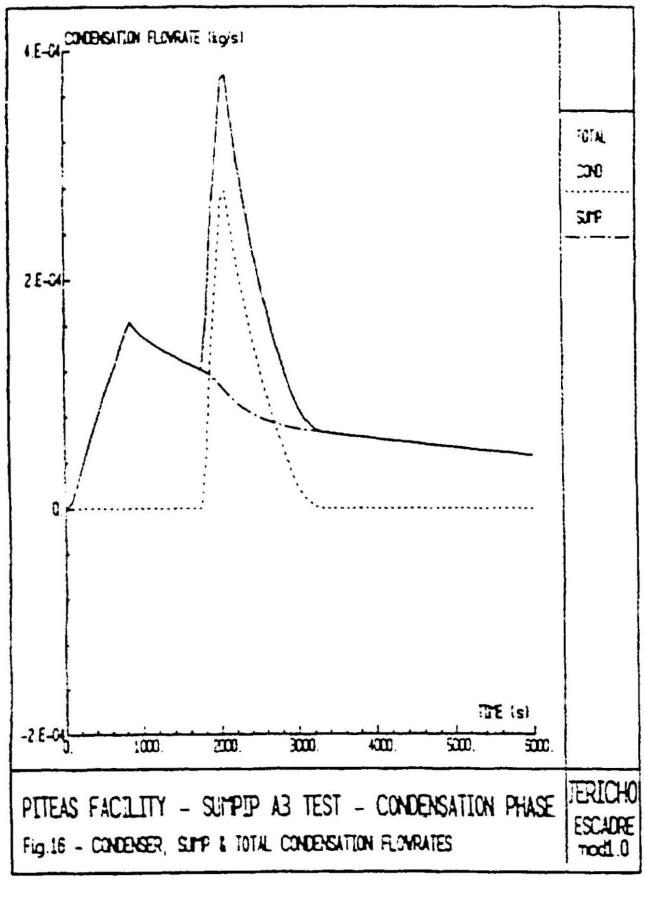


PITEAS FACILITY - SUMPIP A3 TEST - CONDENSATION PHASE

Fig.16 - CONDENSER, SUMP & TOTAL CONDENSATION FLOWRATES

JERICHO
ESCADRE
mod1.0

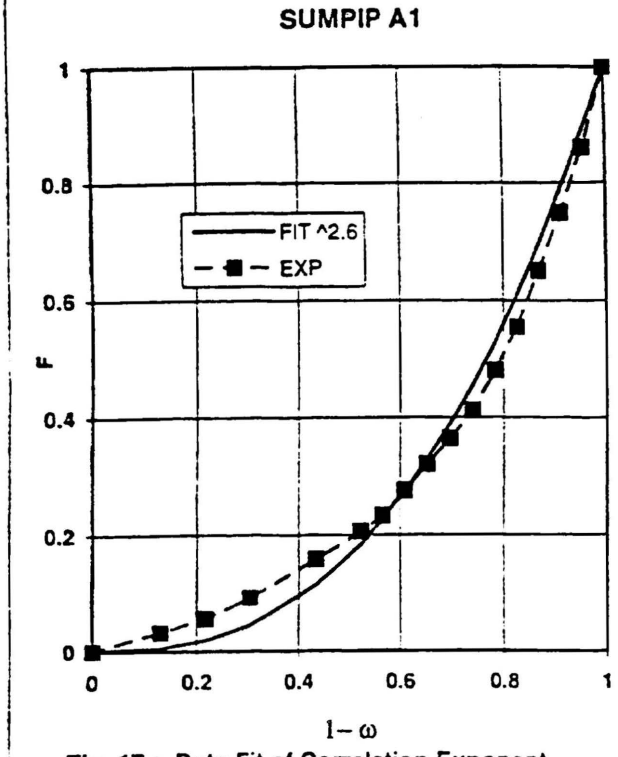


Fig. 17 : Data Fit of Correlation Exponent

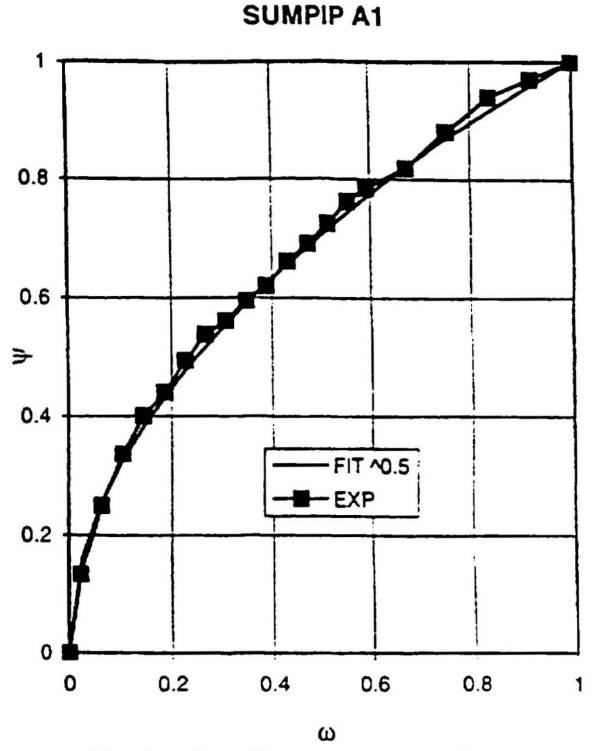


Fig. 18 : Data Fit for PSI Parameter

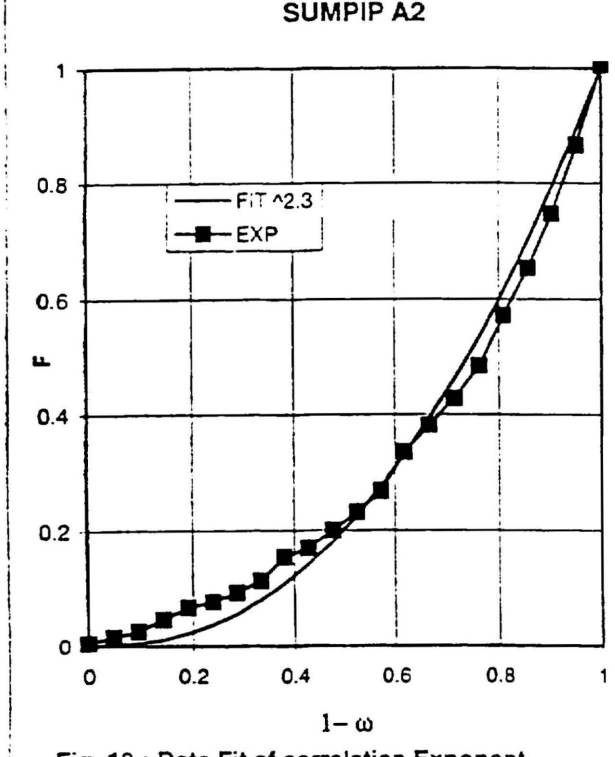


Fig. 19 : Data Fit of correlation Exponent

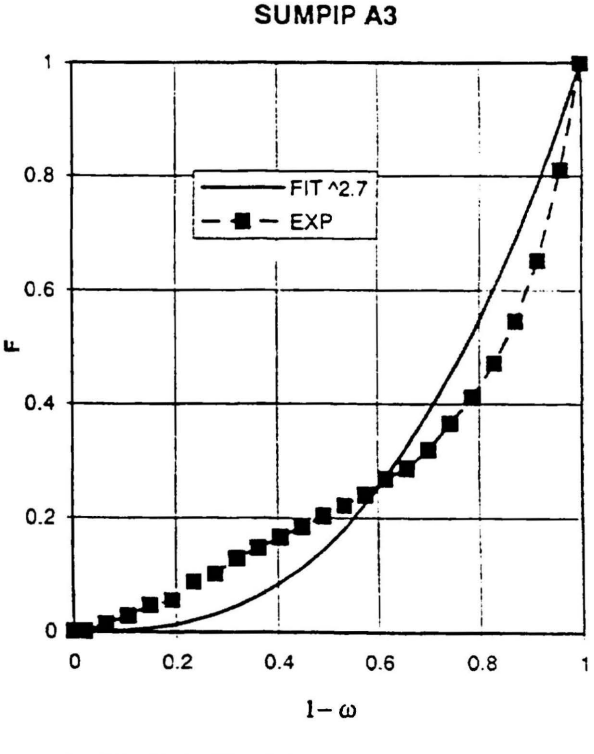


Fig. 20 : Data Fit of Correlation Exponent